Model of Bow Shock and Magnetopause Surfaces

K. Jelínek, Z. Němeček, and J. Šafránková

Charles University, Faculty of Mathematics and Physics, Prague, Czech Republic.

Abstract. The present models describing location and shape of the magnetopause and the bow shock are based on a statistical evaluation of magnetopause and bow shock crossings. The crossings have been usually identified by time consuming visual inspections of plots or by automated methods which are less reliable. In this paper, we present a new automatic method that can be used for identification of both boundaries if several criteria are fulfilled: 1) available magnetic field and plasma data from a solar wind monitor, and 2) measurements of the magnetic field and plasma density from a sounding spacecraft. We used one-minute medians of continuous measurements of these parameters by a particular spacecraft and distinguished three regions – the solar wind, the magnetosheath, and the inner magnetosphere – according to the magnetic field and plasma density ratios. We explain the method, apply its results to Themis observations, and verify them using our set of magnetopause and bow shock crossings observed by the Themis spacecraft.

Introduction

The magnetopause is the obstacle – varying in size and shape – in flow of the solar wind plasma. In early published papers (e.g., *Fairfield* [1971], *Fairfield* [1976], *Formisano et al.* [1979], *Sibeck et al.* [1991], *Petrinec and Russell* [1996], and *Sotirelis and Meng* [1999]), it was found that the upstream dynamic pressure strongly influences the Earth's magnetopause position. In these papers, a dependence of the stand-off position (R) on the dynamic pressure (p_{dyn}) is scaled with sixth root, $R \approx \sqrt[6]{p_{dyn}}$ which is based on an assumption of the dipole Earth magnetic field. In the paper of *Shue et al.* [1997], different scaling is used and it is explained by a change of a magnetosphere cavity that leads to increase of the magnetosphere magnetic pressure near the magnetopause. Furthermore, it was also found that the second parameter driving the position and shape of the magnetopause is the Z-component of the interplanetary magnetic field (IMF) which is a subject of papers of *Sibeck et al.* [1991], *Petrinec et al* [1991], *Petrinec and Russell* [1996] and *Shue et al.* [1997], etc.

The propagation of the solar wind plasma is supersonic and therefore the bow shock rises ahead of the magnetopause. The Earth's bow shock (BS) is the most studied collisionless shock (e.g., *Fairfield* [1971]; *Formisano et al.* [1973]; *Němeček et al.* [1989]; *Burgess* [1995], and references therein). According to these and other papers, the bow shock position depends on the magnetopause position and on the magnetosheath thickness which is a function of the Mach number. The thickness of the magnetosheath is influenced by a curvature of the obstacle, as it was shown in the papers of *Farris and Russell* [1994] and *Russell and Mulligan* [2002] for the magnetosheath of ICMEs.

Up to now, the models describing an actual location and shape of the magnetopause and bow shock as a function of upstream parameters are based on a statistical processing of crossings observed by a single spacecraft and (usually distant) solar wind monitor. This approach implicitly assumes that the downstream parameters are proportional to their upstream values. Such an assumption introduces many inaccuracies when, for example, a strong sudden change of solar wind parameters results in unusual boundary crossings, or multiple crossings following in a short time and this effect negatively influences statistical results. Moreover, a visual inspection of data plots when looking for boundary crossings is time consumable and subjective

and it differs from one author to other, thus it is very difficult to reprocess such data set.

In the present study, we developed a new method of an automatic identification of both boundaries from measurements of the magnetic field and plasma density. We used continuous measurements of these parameters by a sounding spacecraft and distinguished three regions - the solar wind, magnetosheath, and inner magnetosphere according to measured values. We explain the method of data processing and apply its results to the Themis observations.

Data processing

For our method, we take advantage of orbits of five Themis spacecraft that move through all investigated regions - the solar wind (SW), the magnetosheath (MSH), and inner magnetosphere (MS) and computed one-minute medians of the magnetic field magnitude - $|B_{Themis}|$ and density - n_{Themis}. As a solar wind monitor, we used ACE one-minute medians of the magnitude of the magnetic field - $|B_{ACE}|$, density - n_{ACE}, dynamic pressure p_{dyn}, and the plasma velocity v_{ACE}. Finally, we shifted ACE parameters to Themis positions by convection along the X_{GSE} axis.

We applied continuous measurements of the Themis spacecraft from March 2007 to September 2009 and computed the ratio of the magnetic fields, r_B

$$r_B = \frac{|B_{Themis}|}{|B_{ACE}|}. \tag{1}$$

Because the compression ratio of the magnetic field in the MSH decreases towards the flanks, we added the density compression factor, r_n

$$r_n = \frac{n_{Themis}}{n_{ACE}}. \tag{2}$$

These two ratios allowed us to identify three regions: SW, MSH, and MS on whole dayside orbits and even towards the flanks in the range of ± 7 hours of local time around the local noon. It would be more appropriate also to use a similar ratio of the plasma velocity, however, this would reduce the number of usable data to one quarter.

Figure 1 shows 2D histogram of numbers of one-minute measurements binned in r_B and r_n. One can distinguish three regions: solar wind measurements are spread around $r_B = 1$ and $r_n = 1$ (it is not exactly the point because some inaccuracies are created through shifting and comparison of two distant data sources); the magnetosheath is specified by a compression ratio about $r_B \approx 4$ and $r_n \approx 5$ (the magnetosheath has larger spread around these ratios because its parameters strongly depend on a particular position inside the magnetosheath). In the inner

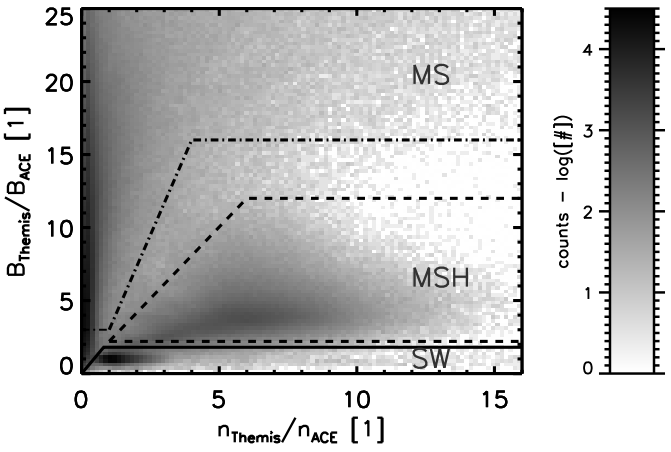

Figure 1. 2D histogram of the ratios of r_B vs r_n which were used to distinguish between three regions – the solar wind is at the bottom, the magnetosphere is located at the left part and the magnetosheath is spread in the middle. Values in the histogram are shown in logarithmic scale.

magnetosphere, the plasma density is smaller than in the solar wind and the magnetic field does not depend on the solar wind magnetic field, thus the ratio can reach high values. It is seen as a long ridge for $r_n < 1$. In Figure 1, we show the chosen boundaries between particular regions. The points which lie outside these boundaries are not used in our processing.

Description of the method

The identification of the bow shock and magnetopause is based on probability that a spacecraft visited a particular region, i.e., that the point with co-ordinates (r_B and r_n) corresponds to one of the regions specified in Figure 1. Assuming the symmetric magnetosphere, we divided the space of investigated parameters (spatial coordinates and dynamic pressure) into particular bins. The dimension of the bins changes along the X_{GSE}; at the nose, the bin dimension is 0.25 x 3 R_E. In every bin, we compute a probability, P that we can find the SW, MSH, and MS in a given position for a given dynamic pressure

$$P_{SW}(p_{dyn}, X, Y) = \frac{N_{SW}(p_{dyn}, X, Y)}{N_{ALL}(p_{dyn}, X, Y)} \quad (3)$$

$$P_{MSH}(p_{dyn}, X, Y) = \frac{N_{MSH}(p_{dyn}, X, Y)}{N_{ALL}(p_{dyn}, X, Y)} \quad (4)$$

$$P_{MS}(p_{dyn}, X, Y) = \frac{N_{MS}(p_{dyn}, X, Y)}{N_{ALL}(p_{dyn}, X, Y)}, \quad (5)$$

where N_{SW}, N_{MSH} and N_{MS} are numbers of one-minute intervals. Note that this set of probabilities can be extended by others quantities like IMF B_Z, Mach number, etc.

There are several possibilities how to identify magnetopause and bow shock positions from this set of computed probabilities. For example, it is possible to find such boundary where the probability of neighboring regions (such as SW and MSH or MSH and MS) is 50%, however, this way is sensitive to missing data or noise. We went another way - we have defined an analytical form (model) describing the bow shock and magnetopause locations and we fitted free model parameters by minimizing chi-square for every their combination.

We suggested that the position of the magnetopause depends on the dynamic pressure as $R_{MP} \approx p^{-\frac{1}{\epsilon}}$, where ϵ is 6 (*Fairfield* [1971]) or 6.667 (*Shue et al.* [1997]), therefore we optimized binning of the dynamic pressure according to formula

$$\Delta p \approx p^{-\frac{1+\epsilon}{\epsilon}}. \quad (6)$$

Since the dayside magnetopause and bow shock have almost parabolic shapes, it is useful to transform their positions from GSE (x, y, z) coordinates to parabolic coordinates (σ, τ, ϕ) by following expressions

$$\tau = \sqrt{\sqrt{x^2 + (\lambda_y y)^2 + (\lambda_z z)^2} - x} \quad (7)$$

$$\sigma = \sqrt{\sqrt{x^2 + (\lambda_y y)^2 + (\lambda_z z)^2} + x} \quad (8)$$

$$\phi = \arctan \frac{\lambda_y y}{\lambda_z z} \quad (9)$$

where λ_y and λ_z are scaling factors. If these factors are chosen by a proper way, the locations of the bow shock and magnetopause would lie on surfaces $\sigma = const$ only in the whole range of the dynamic pressures. Using the least square method, we have found following scaling factors: $\lambda_{y\,BS} = 1.17$ and $\lambda_{y\,MP} = 1.54$. In such a case, model BS and MP positions can be expressed as

$$\sigma = \sqrt{2R_0 p_{dyn}^{-\frac{1}{\epsilon}}} \quad (10)$$

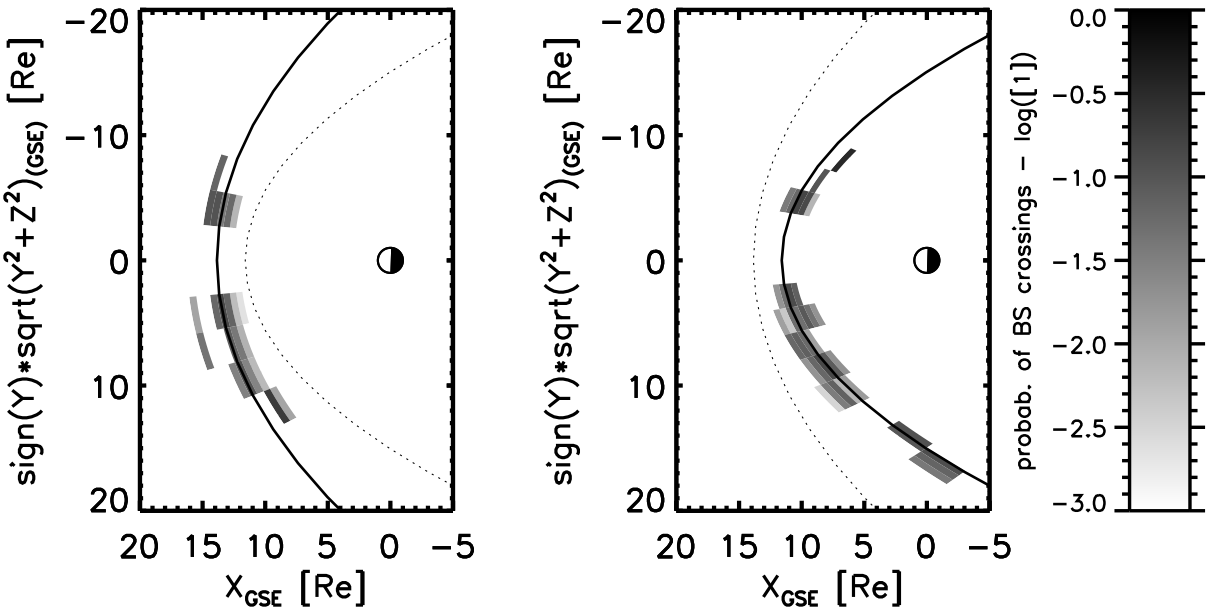

Figure 2. The composed plots of the suggested bow shock (right) and magnetopause (left) model surface (BS – solid line in the left and dotted line in the right parts) and 2D probability of the bow shock (magnetopause) position for a particular bin of the dynamic pressure (from 1.8 nPa to 2 nPa) showed by the gray scale.

where R_0 is the stand-off distance for $p_{dyn} = 1$ and a given scaling factor, ϵ. Another application of the least square method leads to following expressions:

$$R_{MP} = 12.82\, {p_{dyn}}^{-\frac{1}{5.26}} \quad (11)$$

$$R_{BS} = 15.02\, {p_{dyn}}^{-\frac{1}{6.55}} \quad (12)$$

where R_{MP} and R_{BS}, respectively are stand-off subsolar positions of new magnetopause and bow shock model positions. Surprisingly low value of ϵ in the case of the magnetopause can be probably explained by a presence of plasma pressure inside the inner magnetosphere. However, we should note that the recent paper of *Lin et al.* [2010] reports even a lower exponent ($\approx$ 5.15). The expression for the bow shock does not take into account the Mach number, however, the dependence of the bow shock location on the Mach number is rather weak for $M > 4$ and this condition is fulfilled for a majority of the observations.

Validation of the model

The described model was developed using probabilities that the sounding spacecraft visited a particular region and its performance can be tested by a comparison with observed crossings of both boundaries. We have visually identified more than 6000 bow shock and 5500 magnetopause crossings in Themis data in course of the years of 2007 and 2008. Because these sets were biased by the low apogee of the Themis spacecraft, mainly during the first stage of the Themis project (2007), we have developed a method for suppression of this bias (*Jelínek et al.* [2009]). However, in contrast to *Jelínek et al.* [2009] in the present paper we have developed fully automatic method and used parabolic coordinates and nonlinear binning of the solar wind dynamic pressure.

An example of a comparison between bow shock and magnetopause models and positions of observed bow shock (left) and magnetopause (right) crossings can be found in Figure 2. The gray scale shows the probability that the bow shock (magnetopause) crossing was observed in a particular spatial bin and under a given p_{SW} (in Figure 2, p_{SW} was in the range from 1.8 to 2.0 nPa). One can note a good matching of observations and model results. To quantify their

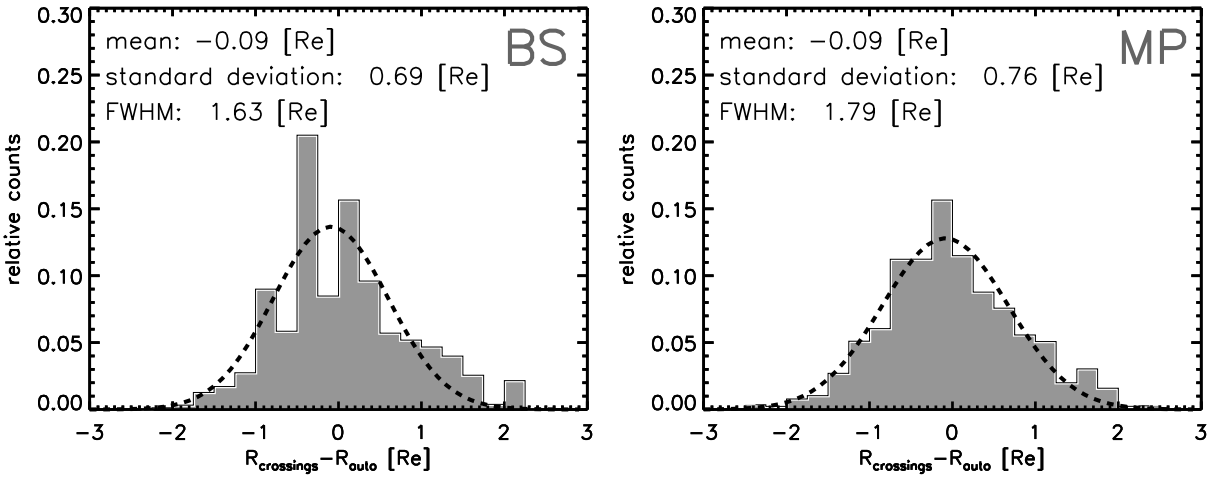

Figure 3. (left) Distributions of differences between positions of observed bow shock crossings and mean positions of the bow shock obtained by the automatic method; (right) The same plot for the magnetopause. The parameters of distributions are marked at the top of each panel. Abbreviation FWHM notes full width at half maximum.

deviations, the histograms in Figure 3 represent the differences between mean positions of the bow shock (left) and the magnetopause (right) determined from boundary crossings and from the proposed model. Both distributions are almost centered and standard deviations are about 0.69 and 0.76 R_E for the bow shock and magnetopause, respectively.

Lin et al. [2010] developed a very complex magnetopause model parametrized with the dynamic pressure, IMF B_Z, and tilt angle. They tested their model as well as several older models using a set of 62 observed low-latitude crossings and found that the values of standard deviations are in a range 0.65-1 R_E and only their model provided standard deviations of 0.54 R_E. From this comparison follows that our result 0.76 R_E is relatively good if we take into account that we incorporate only the dependence on the solar wind dynamic pressure.

Another way to test of our model is to use a similar fitting method as we described above to visually identified MP and BS crossings. Applying this approach, we found stand-off positions of the magnetopause, R_{MP} and bow shock, R_{BS} (in a similar form to equations (11) and (12))

$$R_{MP} = 12.90\, {p_{dyn}}^{-\frac{1}{4.92}} \quad (13)$$

$$R_{BS} = 14.94\, {p_{dyn}}^{-\frac{1}{6.62}}. \quad (14)$$

Comparing both sets of the equations, we can conclude that values R_0 and ϵ are close to the suggested model. This result validates our method but, as mentioned above, the sets of crossings suffer with the orbital bias and it is not clear if the method of *Jelínek et al.* [2009] can remove this bias completely. On the other hand, the method used for the model development in the present paper does not depend on the spacecraft orbits.

Conclusion

We have developed a new automatic method for identifications of BS and MP positions and shapes. We successfully validated this method using by ≈ 6000 BS and ≈ 5500 MP dayside crossings that we have identified by a visual inspection of Themis data plots. Finally, we determined the BS and MP boundaries for the whole dayside magnetosphere in the range of dynamic pressures from 0.6 to 11 nPa.

We found that the automatic method can be used for developing of the magnetopause and bow shock model without identification of boundary crossings. The model is in good agreement with results obtained from observed boundary crossings and its results are comparable with the

previous more complex models. We plan to extend the set of input parameters, especially with IMF B_Z for the magnetopause and the Mach number for the bow shock.

Acknowledgments. The present work was supported by the Charles University Grant Agency under Contract 102508 and partly by Research project MSM0021620860 financed by the Ministry of Education of Czech Republic.

References

Burgess, D., Collisionless Shocks, In: *Introduction to Space Physics, M.G. Kivelson and C.T.Russell (eds)*, Cambridge: *Cambridge University Press*, Chapt. 5, pp. 129-163, 1995.

Fairfield, D.H., Average and unusual location of the Earth's magnetopause and bow shock, *J. Geophys. Res.*, **76**, 6700, 1971.

Fairfield, D.H., A summary of observations of the Earth's bow shock, In: *Physics of Solar Planetary Environments*, pp. 514-527, 1976.

Farris, M. H., and C. T. Russell, Determining the standoff distance of the bow shock: Mach number dependence and use of models, *J. Geophys. Res.*, **99**, 17,681-17,689, 1994.

Formisano, V., G. Hedgecock, G. Moreno, F. Palmiotto, and J.K. Chao, Solar wind interaction with the Earth's magnetic field, 2, Magnetohydrodynamics bow shock, *J. Geophys. Res.*, **87**, 3731, 1973.

Formisano, V., V. Domingo, K.-P. Wenzel, The tree-dimensional shape of the magnetopause, *Planet. Space Sci.*, **27**, 1137-1149, 1979.

Jelínek, K., Z. Němeček, J. Šafránková, Themis: Locations of dayside bow shock and magnetopause, *in WDS'09 Proceedings of Contributed Papers: Part II – Physics (eds. J. Safrankova and J. Pavlu), Prague, Matfyzpress*, pp. 1521, 2009.

Lin, R.L., X.X. Zhang, S.Q. Liu, Y.L. Wang, and J.C. Gong, A three-dimensional asymmetric magnetopause model, *J. Geophys. Res.*, **115**, A04207, doi:10.1029/2009JA014235, 2010.

Němeček, Z., J. Šafránková and G. Zastenker, Dynamics of the bow shock position, *Adv. Space Res.*, **8**, No. 9-10, (9)167-(9)170, 1989.

Petrinec, S.M., P. Song, and C.T. Russell, Solar cycle variation in the size and shape of the magnetopause, *J. Geophys. Res.*, **96**, 7893, 1991.

Petrinec, S.M., C.T. Russell, Near-Earth magnetotail shape and size as determined from the magnetopause flaring angle, *J. Geophys. Res.*, **101**, 137, 1996.

Russell, C.T and T. Mulligan, On the magnetosheath thicknesses of interplanetary coronal mass ejections, *Planet. Space Sci.*, **50**(5/6), 527-534, 2002.

Shue, J.-H., J.K Chao, H.C. Fu, C.T. Russell, P.Song, K.K. Khurana, and H.J. Singer, A new functional form to study the solar wind control of the magnetopause size and shape, *J. Geophys. Res.*, **102**, 9497-9511, 1997.

Sibeck, D.G., R.E. Lopez, E.C. Roelof, Solar wind control of the magnetopause shape, location, and motion, *J. Geophys. Res.*, **96**, 5489-5495, 1991.

Sotirelis, T. and C. T. Meng, Magnetopause from pressure balance, *J. Geophys. Res.* **104**, 6889, 1999.